THE JOURNAL OF PHYSICAL CHEMISTRY A

ARTICLE

pubs.acs.org/JPCA

Angular Intensity Distribution of a Molecular Oxygen Beam Scattered from a Graphite Surface

Junepyo Oh,[†] Takahiro Kondo,[*,†] Keitaro Arakawa,[†] Yoshihiko Saito,[†] W. W. Hayes,[‡,§] J. R. Manson,[‡] and Junji Nakamura[†]

[†]Graduate School of Pure and Applied Science, University of Tsukuba, 1-1-1 Tennoudai, Tsukuba, Ibaraki 305-8573, Japan

[‡]Department of Physics and Astronomy, Clemson University, Clemson, South Carolina 29634, United States

[§]Physical Sciences Department, Greenville Technical College, Greenville, South Carolina 29606, United States

ABSTRACT: The scattering of the oxygen molecule from a graphite surface has been studied using a molecular beam scattering technique. The angular intensity distributions of scattered oxygen molecules were measured at incident energies from 291 to 614 meV with surface temperatures from 150 to 500 K. Every observed distribution has a single peak at a larger final angle than the specular angle of 45° which indicates that the normal component of the translation energy of the oxygen molecule is lost by the collision with the graphite surface. The amount of the energy loss by the collision has been roughly estimated as about 30−41% based on the assumption of the tangential momentum conservation during the collision. The distributions have also been analyzed with two theoretical models, the hard cubes model and the smooth surface model. These results indicate that the scattering is dominated by a single collision event of the particle with a flat surface having a large effective mass. The derived effective mass of the graphite surface for the incoming oxygen is 9−12 times heavier than that of a single carbon atom, suggesting a large cooperative motion of the carbon atoms in the topmost graphene layer

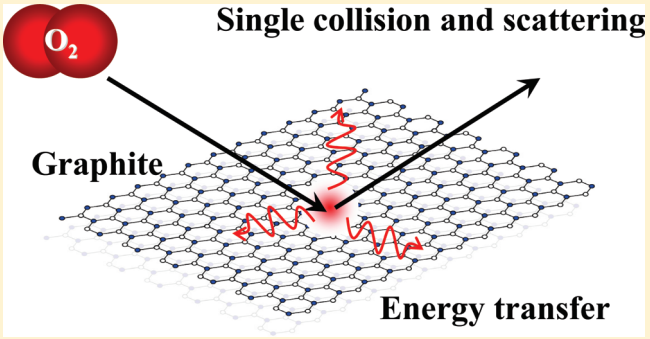

1. INTRODUCTION

The interaction between oxygen molecules and graphite-related materials is of fundamental interest to understanding processes of burning phenomena in nature. Depending on the interaction condition with oxygen, graphite-related materials are also known to show superior catalytic activity such as for the oxygen reduction reaction in fuel cells.[1] It is thus important to understand the interaction between an oxygen molecule and the graphite surface for the efficient usage of the graphite-related materials. In this work, we have analyzed the energy transfer process of oxygen with the graphite surface under a wide variety of collision conditions. The collision is an initial important interaction process of all of the chemical and catalytic activities. During the collision, parts of the translational and internal energy of the oxygen molecule are transferred to the surface through multiple phonon creation and/or electron−hole pair excitation. Excitations of the internal degrees of freedom and/or translational energy of oxygen are also expected to occur through phonon annihilations at the graphite surface. Depending on these energy transfer processes, the oxygen molecules can adsorb on the graphite surface followed by the reaction with carbon atoms or they are scattered from the surface. The energy transfer process thus decides the fates of oxygen and the graphite surface after the collision.

The graphite surface is known to have large anisotropy in the thermal properties between parallel and perpendicular to the *c*-axis of the crystal[2] because it is made from stacking of two-dimensional hexagonal lattices with weak interlayer interaction. When a Xe atom collides with the graphite surface, the topmost graphene layer has been reported to behave as a "trampoline" due to the cooperative motion of carbon atoms.[3,4] The cooperative motion is considered to be governed by the C−C bonds composed of σ-bonds and π conjugated system of the graphite surface.[5] In the case of oxygen, a similar scattering process like Xe is expected to occur due to its having a heavier mass than carbon. In addition, oxygen has extra degrees of internal freedom in comparison to the Xe atom. It is thus expected that a wide variety of scattering processes will be observed in the case of oxygen scattering from graphite.

In this work, in order to clarify some of the scattering features of oxygen in detail, we have measured angular intensity distributions of oxygen molecules scattered from the graphite surface under a wide range of collision conditions by applying the supersonic molecular beam scattering technique. The results were then analyzed with two theoretical model calculations, the hard cubes model,[6] and the more recently developed smooth

Special Issue: J. Peter Toennies Festschrift

Received: December 30, 2010
Revised: February 25, 2011
Published: March 29, 2011

surface model.[7] Despite the large mass and additional internal degrees of freedom of oxygen, the scattering process is found to be well reproduced by the single collision event of the particle with the flat surface having a large effective mass.

2. EXPERIMENT

The experimental apparatus used for molecular beam scattering has already been described elsewhere.[8,9] The apparatus consists of five stainless-steel chambers. Each chamber is independently pumped to ultrahigh vacuum (UHV). A supersonic O_2 (10% oxygen seeded in He) beam is generated by free-jet expansion from a pinhole in a cylindrical nozzle and skimmed using a conical skimmer. The diameter of the nozzle pinhole is set to 0.05 mm. Stagnation pressure in the nozzle is controlled by a commercial gas regulator from 1 to 100 atm. The translational energy E_i of the molecular beam is controlled by heating the nozzle temperature T_n from 300 to 700 K within a temperature fluctuation of ±0.1 K. T_n is monitored by a type-K (chromel/alumel) thermocouple spot-welded at the edge of the nozzle near the pinhole. The impinging molecules are reflected from graphite in the scattering chamber and are detected by a quadrupole mass spectrometer (ULVAC MSQ-400) in the detector chamber. The energy spread $\Delta E_i/E_i$ of the molecular beam used in this study is less than 20%. The detailed profiles of the molecular beam were measured by the time-of-flight technique.

The sample surface of highly oriented pyrolytic graphite (HOPG, ZYA-grade, Panasonic, 12 mm × 12 mm × 1.5 mm) was cleaved in air by adhesive tape and then put into a UHV chamber. The HOPG sample was mounted on a sample holder which can be cooled down to 90 K by a cryogenic refrigerator head (Iwatani CryoMini S050) and can be heated by infrared radiation from a hot W filament placed close to the back side of the HOPG sample. The surface temperature of HOPG was measured by a type-K thermocouple attached on the edge of the sample surface by a Ta clamp. Prior to the experiment, the HOPG sample was annealed at 800 K in UHV for 5 min in order to clean the surface.

After heat treatment, the angular intensity distribution measurement is carried out for oxygen molecules scattered from the graphite surface by rotating the sample along the axis perpendicular to the beamline with an accuracy of ±0.1°. Throughout the present study, both incident and scattering angles are defined with respect to the surface normal direction. The sum of the incident and scattering angles was fixed at 90°. No detector sensitivity corrections were made for our obtained intensity distributions.

To examine the degree of energy loss quantitatively, we have roughly estimated the amount of energy loss of the oxygen molecules by using the concept of the HCM.[6] According to the major HCM assumption, the tangential component of momentum of the incident atom is conserved during the single collision event with the surface (this is known as "tangential momentum conservation"). Using this assumption and experimentally observed angular intensity distributions, we can roughly estimate the most probable amount of energy loss during the collision under each collision condition. Figure 1 shows the schematic of the analyzed scattering geometry. The subscripts "i" and "f" indicate the *incident* and *scattered* components, respectively. θ_i is the incident angle, θ_f the scattering angle, E_i the energy of incident molecule, and E_f is the energy of a scattered molecule. The subscripts "⊥" and "∥" indicate the perpendicular and parallel components, respectively. As shown in Figure 1, the sum of the incident and scattering angles has been fixed to 90° in our experimental conditions, i.e., $\theta_i + \theta_f = 90°$. The perpendicular and parallel contributions to the incident energy can thus be represented by following simple equations

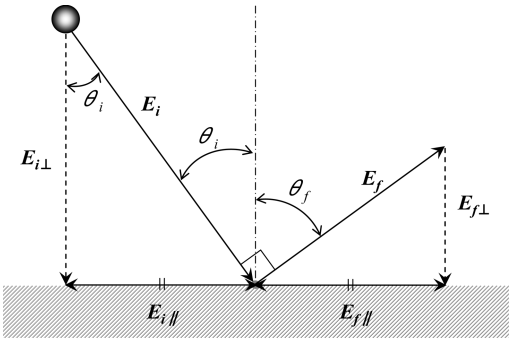

Figure 1. Schematic of the energy loss calculation using the concept of the HCM. The tangential component of momentum of the incident atom is conserved during the single collision event with the surface ($E_{f\parallel} = E_{i\parallel}$) and the sum of the incident and scattering angles is fixed at 90°.

$$E_{i\perp} = E_i \cos^2 \theta_i \quad (1)$$

$$E_{i\parallel} = E_i \sin^2 \theta_i \quad (2)$$

Owing to the tangential momentum conservation in the HCM, $E_{f\parallel}$ is the same as $E_{i\parallel}$, while the perpendicular component of scattering energy $E_{f\perp}$ is represented as follows

$$E_{f\perp} = E_i \sin^2 \theta_i \tan^2 \theta_i \quad (3)$$

The value of $(1 - E_f/E_i)$ gives an estimate of the energy loss of oxygen molecules by the collision with the graphite surface.

3. THEORETICAL CALCULATION

3.1. Hard Cube Model. In order to understand the scattering event, we have used a simple classical binary collision model of the hard cube model (HCM). In this model, gas-molecule scattering is represented by a classical binary collision of a hard sphere (gas atom) and a cube (surface atoms) with effective surface mass with an initial velocity v chosen from a Maxwellian distribution corresponding to the surface temperature T_S. The hard wall interaction potential between gas and cube is assumed to be flat with no corrugation, and the tangential component of the momentum of the incoming atom is conserved upon scattering. Although the model oversimplifies the scattering events, qualitative insights into the scattering event can be derived. The intensity of the scattered projectile, I_{HCM}, is explicitly described[6] as

$$I_{HCM} = \frac{1}{u_{i\perp}} \int_0^\infty (\cos \theta_i + B_1) B_2 u_i^2 F_i(u_i) G_i(B_1 u_i)\, du_i \quad (4)$$

where u_i is the velocity of the incident He beam, $u_{i\perp}$ the normal component of u_i, θ_i the incident angle of the He beam, $F_i(u_i)$ and $G_i(B_1 u_i)$ are the velocity distributions of the incident He beam and surface atom, respectively. B_1, B_2, and $G(B_1 u_i)$ are described as follows

$$B_1 = \frac{1+\mu}{2} \sin \theta_i \cot \theta_f - \frac{1-\mu}{2} \cos \theta_i \quad (5)$$

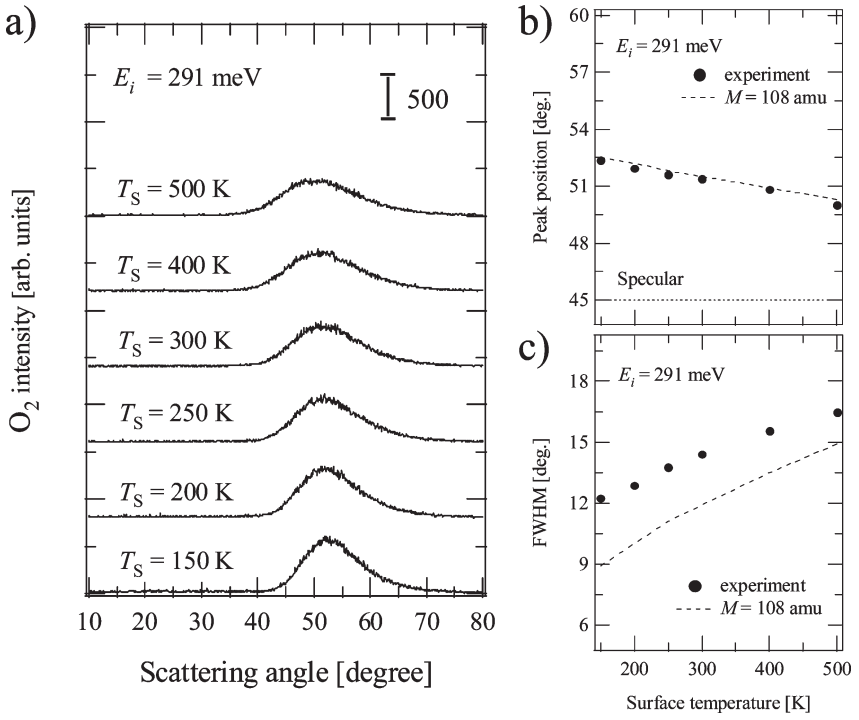

Figure 2. (a) The surface temperature dependence of the angular intensity distribution of oxygen molecules (E_i = 291 meV) scattered from a graphite surface. (b) The peak position and (c) width (full width at half-maximum, fwhm) of the O_2 scattering distribution as a function of the surface temperature. The dashed line indicates the results of the hard cubes model (HCM) calculation with effective mass (M) of 108 amu.

$$B_2 = \frac{1+\mu}{2} \sin\theta_i \csc^2\theta_f \tag{6}$$

$$G(B_1 u_i)\, dv_i = \left(\frac{M}{2\pi k_B T_S}\right)^{1/2} \exp\left(-\frac{M}{2k_B T_S}(B_1 u_i)^2\right) d(B_1 u_i) \tag{7}$$

where μ is the ratio of the mass m of O_2 and the effective mass M of the surface, k_B is Boltzmann's constant, and $B_1 u_i$ represents the velocity of the surface atom.

3.2. Smooth Surface Model. Hayes and Manson have utilized analytical descriptions to represent inelastic surface scattering of atomic and molecular projectiles using classical scattering theory,[7] the so-called smooth surface model (SSM). The model includes internal degrees of freedom of the molecule, and thus one can access the information about the energy transfer process with the rotational and vibrational motions of the molecule during the collision. The theory is based on the classical mechanical model for surface scattering developed by Brako and Newns[10] with a scattering form factor for a hard repulsive interaction potential.[11,12] This describes scattering from a flat potential energy surface with vibrationally induced corrugation caused by vibrational motions of the underlying atoms. This theory has proven to be useful in explaining the energy-resolved spectra and angular intensity distributions of rare gas atoms scattering from molten metal surfaces[7] and has been useful in describing He and Ar scattering from graphene and C_{60} layers on a Pt(111) substrate.[13] Extensions of this theory to molecular scattering from surface have also been reported for methane scattering from LiF(001) and Pt(111).[14,15] In the smooth surface model, the differential reflection coefficient for an atomic projectile is given as

$$\frac{dR}{d\theta_f\, dE_f} = \frac{m^2 v_R{}^2 |\vec{u}_f|}{8\pi^3 \hbar^2 u_{i\perp} S_{uc}} |\tau_{fi}|^2 \left(\frac{\pi}{k_B T_S \Delta E_0}\right)^{3/2} \exp\left(-\frac{(E_f - E_i + \Delta E_0)^2 + 2v_R{}^2 m^2 (u_{f\parallel} - u_{i\parallel})^2}{4k_B T_S \Delta E_0}\right) \tag{8}$$

where S_{uc} is the unit cell area associated with a single surface atom and v_R is a parameter having dimensions of speed that is completely determined by the phonon spectral density at the surface. ΔE_0 is the recoil energy which includes the surface effective mass M, given by $\Delta E_0 = m^2 (\vec{u}_f - \vec{u}_i)^2/2M$, and $|\tau_{fi}|^2$ is a form-factor determined by the interaction potential.

In a classical mechanical derivation of eq 8 the quantity $\hbar$ is a constant having dimensions of action, but a derivation starting from quantum mechanics and then taking the classical limit identifies this quantity as Planck's constant divided by 2π.

4. RESULTS

4.1. Angular Intensity Distributions. We measured angular intensity distributions of an oxygen molecular beam scattered from a graphite surface as functions of surface temperature (T_S) and incident energy (E_i). Figure 2a shows the T_S dependence of the distributions at E_i = 291 meV. In every case, the distribution has a single peak at around 52° and has a broader width than that in the case of atom scattering such as He and Ar.[5,16] The peak is positioned at scattering angles larger than 45° indicating that the normal component of the translation energy of the oxygen

dx.doi.org/10.1021/jp112394m |J. Phys. Chem. A 2011, 115, 7089–7095

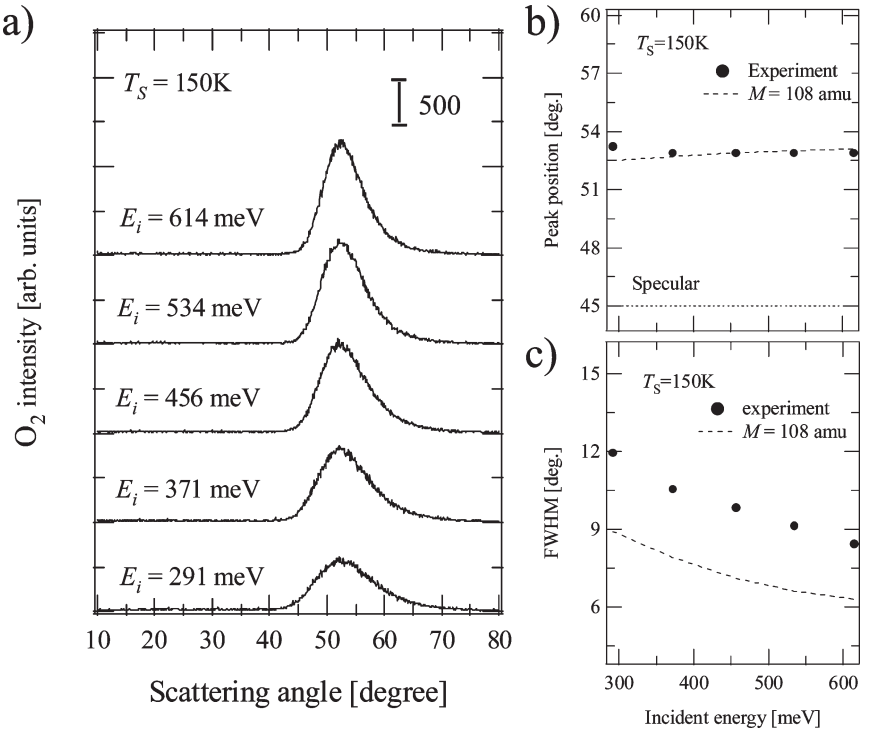

Figure 3. (a) The incident energy dependence of the angular intensity distribution of oxygen molecules scattered from a graphite surface. (b) The peak position and (c) fwhm of the O_2 scattering distribution. The dashed line indicates the results of the HCM calculation with effective mass (M) of 108 amu. The surface temperature is 150 K.

molecule was reduced by the collision with the graphite surface. Broader width of the distribution indicates various types of energy transfer process in the case of scattering of O_2 from graphite.

Panels b and c of Figure 2 show the peak position and width (full width at half-maximum, fwhm) of the O_2 scattering distribution as a function of the surface temperature. As shown in Figure 2b, the peak shifts toward lower scattering angles with the increase of the surface temperature. This result suggests that the energy loss of the oxygen molecules by the collision with the graphite surface becomes smaller at higher surface temperature. This can be interpreted as due to the increased motion of the surface atoms at higher surface temperatures, i.e., the velocity of the surface carbon atoms colliding with the incoming oxygen molecules becomes larger with the increase of the surface temperature. The larger velocity distribution of the surface carbon atoms also leads to a broader fwhm at higher T_S as shown in Figure 2c. These tendencies are well reproduced by the hard cubes model. The dashed line in the figure shows the calculated results using the HCM, where the effective mass of the surface is selected as M = 108 amu to reproduce the experimentally observed peak position. The effective mass of M = 108 amu corresponds to the mass of nine carbon atoms. The surface effective mass derived by fitting experimental data is often greater than the single atomic mass in many theoretical model analyses,[5,8,14−30] which is attributed to the cooperative motion of the surface atoms.[3] Contrary to the case of peak positions, a larger deviation is observed between experimental results and calculated results in the peak width. The experimental peak widths are broader than those of HCM calculation when effective mass is set as M = 108 amu. This deviation is considered to be caused by the effects of the internal energy of oxygen molecules such as rotational energy excitation by the collision which is not included in the HCM.

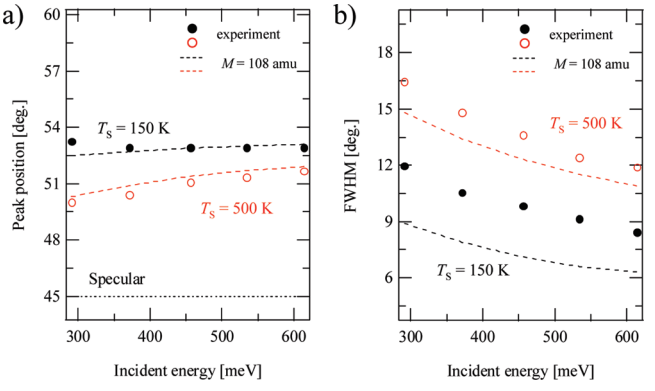

Figure 4. Comparison of the incident energy dependence of molecular oxygen beam scattering performed at T_S = 150 K and T_S = 500 K. (a) peak position, and (b) fwhm of the O_2 scattering distribution. In each panel, black circles and dashed lines indicate the results of experiment and HCM calculations (M = 108 amu) at T_S = 150 K, and red circles and dashed lines indicate the results of experiment and HCM calculations (M = 108 amu) at T_S = 500 K.

The incident energy dependence of the angular intensity distribution of the oxygen molecules scattered from graphite surface at 150 K is shown in Figure 3 together with the predictions based on the hard cubes model. In every case, the peak is also positioned at a larger scattering angle than 45° and has a broad distribution width. The peak position calculated by the HCM again well reproduces the incident energy dependence as shown in Figure 3b. The best fitting results for the peak position are obtained when the effective mass is set to M = 108 amu as in the case of the surface temperature dependence. However, a

dx.doi.org/10.1021/jp112394m |J. Phys. Chem. A 2011, 115, 7089–7095

Table 1. The Roughly Estimated Energy Loss of Oxygen Molecules for All Angular Intensity Distribution Spectra as Functions of Both Surface Temperature T_S and Incident Energy E_i[a]

	dependence of surface temperature						dependence of incident energy				
T_S (K)	150	200	250	300	400	500	150 (500)				
E_i (meV)	291						291	371	456	534	614
θ_f(deg)	52.4	51.9	51.6	51.4	50.8	50	52.4 (50)	52.3 (50.4)	52.3 (51.1)	52.4 (51.3)	52.4 (51.7)
θ_i(deg)	37.6	38.1	38.4	38.6	39.2	40	37.6 (40)	37.7 (39.6)	37.7 (38.9)	37.6 (38.7)	37.6 (38.3)
$E_{i\perp}$ (meV)	182.5	180.4	178.7	177.7	174.9	170.8	182.5 (170.8)	232.1 (220.3)	285.2 (275.9)	335 (325.5)	385.2 (377.9)
$E_{f\perp}$ (meV)	64.5	67.8	70.5	72.3	77.1	84.6	64.5 (84.6)	83.2 (103)	102.2 (117.5)	118.2 (133.5)	135.9 (147.4)
energy loss (%)[b]	41	39	37	36	34	30	41 (30)	40 (32)	40 (35)	41 (36)	41 (38)

[a] The values in parentheses indicate the results at T_S = 500 K. [b] The percentage of energy loss are calculated by $(1 - E_f/E_i)\times 100$.

deviation is also observed between experimental results and calculations in the peak width. Contrary to the results for the dependence of surface temperature measurements in Figure 2, the peak position is located at almost the same scattering angle in all distributions. This result suggests that the fraction of energy loss of the oxygen molecules during the collision is insensitive to the incident translational energy in the measured energy range of 291−614 meV. In other words, surface temperature is the dominant factor determining the degree of energy loss under these conditions.

To examine the influence of the surface temperature and incident energy more in detail, the peak position and width of the experimentally observed angular intensity distributions at T_S = 500 K are plotted as a function of E_i in Figure 4 in order to compare with the results at T_S = 150 K and the HCM calculations. The peak positions of the distribution at T_S = 500 K are again well reproduced by the HCM calculation with an effective mass of M = 108 amu. The peak position is shifted toward larger scattering angles with increasing incident energy in the case of T_S = 500 K, i.e., the degree of energy loss is not completely insensitive to the incident energy at T_S = 500 K contrary to the case at T_S = 150 K. Note that all T_S and E_i dependencies in Figures 2b, 3b, and 4a are well reproduced by the simple HCM calculation.

4.2. Amount of Energy Loss in the Collision. The derived energy loss from eq 3 is summarized in Table 1. In the case of the dependence on surface temperature, the energy loss decreases from 41% to 30% with the increase of surface temperature from 150 to 500 K. Contrary to the dependence on surface temperature, the energy loss shows almost the same amount of 40−41% for the incident energy dependence at T_S = 150 K as expected from the peak position angles in Figure 3b. Note that this amount of energy loss is the maximum energy loss our experimental conditions. For the results at T_S = 500 K, the amount of energy loss changed from 30% to 38% with the increase of incident energy of oxygen molecules. These results quantitatively indicate that the energy loss of the oxygen molecules was governed by both the surface temperature and incident energy of oxygen except for the specific scattering conditions (T_S = 150 K).

5. DISCUSSION

An oxygen molecule is heavier than a carbon atom, and thus one might expect that the oxygen molecule would be trapped on the graphite surface after the collision due to its heavier mass according to the concept of a simple classical binary collision. That is, parts of the energy of the oxygen molecule should be transferred to the carbon atom in the initial collision and then the oxygen molecule should continue in a forward direction. If such a

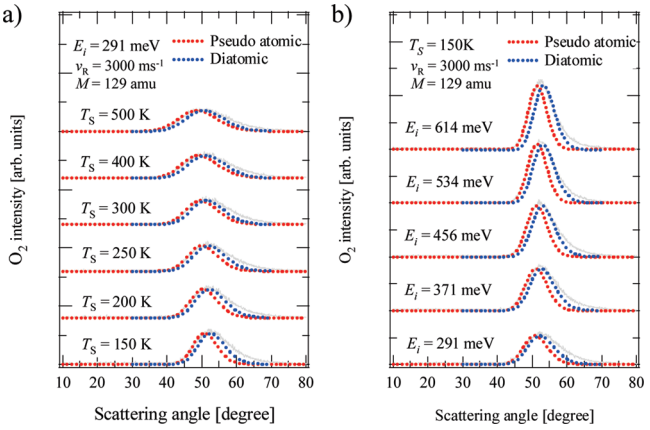

Figure 5. The analytical fitting results of the angular intensity distribution of oxygen molecules scattered from a graphite surface as functions of (a) surface temperature T_S and (b) incident energy E_i using the smooth surface model (SSM). The gray solid line is experimental data; red dotted points indicate the result when the incident oxygen molecules are considered as pseudoatomic, and blue dotted points indicate the result when the incident oxygen molecules are considered as a rigid diatomic projectile.

trapping process dominantly takes place, the scattering distribution should consist of multiple scattering components and/or thermally desorbed cosine components. However, the agreement between experimental results and the HCM calculations (Figures 2−4) in peak position angles clearly indicates that the scattering of oxygen from the graphite surface is dominated by a single scattering process such as described by the HCM. In other words, the general scattering features and degree of energy transfer for oxygen scattering from graphite can be interpreted by a simple classical binary collision model with the concept of an effective mass of the surface atom, as in the case of lighter atom/molecule scattering from metal surfaces.[19,20,23,24] In this manner, a relatively small amount of energy loss (30−41%) is estimated for the oxygen upon the collision with graphite as shown in Table 1. This small amount of energy loss supports the concept of an effective surface mass. The difference between the HCM and the experimental results appears only as the broad distribution width in the experimental results, probably due to the effect of the internal energy of the oxygen molecule which is not included in HCM.

Effects of the internal modes of the oxygen molecule on the scattering can be seen from the calculation results of the smooth surface model (SSM). Figure 5 shows the calculated results for all

dx.doi.org/10.1021/jp112394m |J. Phys. Chem. A 2011, 115, 7089–7095

angular intensity distributions as functions of both surface temperature T_S and incident energy E_i using the SSM. In the model calculations, the incident oxygen molecules are considered either as a "pseudoatomic" or a "rigid diatomic" projectile. The value of the effective surface mass is taken to be 1.8 graphite rings (129 amu, 11.75 carbon atoms) and v_R is 3000 m/s for all calculations. As shown in Figure 5, when calculations are carried out by considering oxygen as a rigid diatomic the calculations reproduce the experiment much better than for the case of a pseudoatomic projectile. The SSM calculation thus suggests the following two points: (1) oxygen scattering from graphite is dominated by single scattering events as discussed in the above, and (2) the inclusion of the internal rotational mode of oxygen molecules is needed to accurately reproduce the experimental results. This same conclusion has also been indicated by applying a different diatomic scattering calculation using the simple ellipsoid-washboard model (EWM)[31] (not shown here). However, even including the internal rotational mode of oxygen, the experimental results are not perfectly reproduced by the SSM or EWM for the widths of the distributions (fwhm). In particular, disagreement is significant at larger scattering angles, where the experimental data exhibit larger intensity than that predicted by the calculations. As suggested by our previous work,[16] this enhanced intensity observed in the data at supraspecular angles may be due to effects of defects on the graphite surface, which is not included in the SSM and EWM. To further discuss quantitatively the energy transfer process of oxygen with the graphite surface as well as the cooperative motion of the carbon atoms, measurements of the translational and internal energies of the scattered oxygen molecule are required. By applying time-of-flight and resonance enhanced multiphoton ionization techniques, this will be studied in future work.

6. CONCLUSIONS

We have measured angular intensity distributions of molecular oxygen beams scattered from the highly oriented pyrolytic graphite (HOPG) surface in order to investigate the energy transfer between oxygen molecules and the graphite surface. The angular intensity distributions of scattered oxygen molecules have been measured under various incident beam energies E_i (291 to 614 meV) and surface temperature T_S (150−500 K). In every case, the peak position which indicates the most probable final scattering angle is positioned at a larger scattering angle than 45°. This means that the normal component of the translation energy of the oxygen molecule was reduced by the collision with the graphite surface. The derived energy loss obtained by assuming tangential momentum conservation was about 30−41% in our experimental conditions. This relatively small amount of energy loss can be ascribed to the results of the cooperative motion of the carbon atoms of the topmost graphene layer of the graphite surface.

The peak position angles of the experimentally observed distributions are well reproduced by the hard cubes model and the smooth surface model. The derived effective masses of the graphite surface from each model are M = 108 amu and M = 129 amu, respectively. The agreement of the experimental results with these model calculations suggests that the dominant collision process of an oxygen molecule with the graphite surface can be described by a single scattering of a particle with a surface having an effective mass much (9−12 times) larger than the mass of a single carbon atom. The deviations of the model calculation from the experimental results for the distribution widths are ascribed to the effects of internal modes of the oxygen molecule during the collision such as rotational mode excitation, as well as to the effects of the defects on the graphite surface.

■ ACKNOWLEDGMENT

We appreciate financial support from NEDO (New Energy and Industrial Technology Development) and from the Japanese Ministry of Education, Culture, Sports, Science and Technology (MEXT), under the Grant-in-Aid for Young Scientists (B) 21760023.

■ REFERENCES

(1) Gong, G.; Du, F.; Xia, Z.; Durstock, M..; Dai, L. *Science* **2009**, *323*, 760. Huang, S. F.; Terakura, K.; Ozaki, T.; Ikeda, T.; Boero, M.; Oshima, M.; Ozaki, J.; Miyata, S. *Phys. Rev. B* **2009**, *80*, 235410. Higgins, D.; Chena, Z.; Chen, Z. *Carbon* **2010**, *48*, 3057. Qu, L.; Liu, Y.; Baek, J. B.; Dai, L. *ACS Nano* **2010**, *4*, 1323. Chokai, M.; Taniguchi, M.; Moriya, S.; Matsubayashi, K.; Shinoda, T.; Nabae, Y.; Kuroki, S.; Hayakawa, T.; Kakimoto, M.; Ozaki, J.; Miyata, S. *J. Power Sources* **2010**, *195*, 5947. Lyth, S. M.; Nabae, Y.; Moriya, S.; Kuroki, S.; Kakimoto, M.; Ozaki, J.; Miyata, S. *J. Phys. Chem. C* **2009**, *113*, 20148.

(2) Gurney, R. W. *Phys. Rev.* **1952**, *88*, 465. DeSorbo, W.; Tyler, W. W. *J. Chem. Phys.* **1953**, *21*, 1663.

(3) Grimmelmann, E. K.; Tully, J. C.; Cardillo, M. J. *J. Chem. Phys.* **1980**, *72*, 1039.

(4) Watanabe, Y.; Yamaguchi, H.; Hashinokuchi, M.; Sawabe, K.; Maruyama, S.; Matsumoto, Y.; Shobatake, K. *Chem. Phys. Lett.* **2005**, *413*, 331.

(5) Oh, J; Kondo, T.; Hatake, D.; Nakamura, J. *Surf. Sci.* **2009**, *603*, 895.

(6) Logan, R. M.; Stickney, R. E. *J. Chem. Phys.* **1966**, *44*, 195.

(7) Hayes, W. W.; Manson, J. R. *Phys. Rev. B* **2006**, *74*, 073413. Hayes, W. W.; Manson, J. R. *J. Chem. Phys.* **2007**, *127*, 164714. Ambaye, H.; Manson, J. R. *J. Chem. Phys.* **2006**, *125*, 084717.

(8) Kondo, T.; Kato, H. S.; Yamada, T.; Yamamoto, S.; Kawai, M. *Eur. Phys. J. D* **2006**, *38*, 129.

(9) Kondo, T.; Kato, H. S.; Bonn, M.; Kawai, M. *J. Chem. Phys.* **2007**, *127*, 094703.

(10) Brako, R.; Newns, D. M. *Phys. Rev. Lett.* **1982**, *48*, 1859. Brako, R.; Newns, D. M. *Surf. Sci.* **1982**, *117*, 422.

(11) Muis, A.; Manson, J. R. *J. Chem. Phys.* **1997**, *107*, 1655.

(12) Muis, A.; Manson, J. R. *J. Chem. Phys.* **1999**, *111*, 730.

(13) Yamada, Y.; Sugawara, C.; Satake, Y.; Yokoyama, Y.; Okada, R.; Nakayama, T.; Sasaki, M.; Kondo, T.; Oh, J.; Nakamura, J.; Hayes, W. W. *J. Phys.: Condens. Matter* **2010**, *22*, 304010.

(14) Moroz, I.; Manson, J. R. *Phys. Rev. B* **2004**, *69*, 205406.

(15) Moroz, I.; Manson, J. R. *Phys. Rev. B* **2005**, *71*, 113405.

(16) Oh, J.; Kondo, T.; Hatake, D.; Honma, Y.; Arakawa, K.; Machida, T.; Nakamura, J. *J. Phys.: Condens. Matter* **2010**, *22*, 304008.

(17) Kondo, T.; Tomii, T.; Yamamoto, S. *Chem. Phys.* **2006**, *320*, 140.

(18) Velic, D.; Levis, R. J. *Chem. Phys. Lett.* **1997**, *269*, 59.

(19) Kondo, T.; Okada, R.; Mori, D.; Yamamoto, S. *Surf. Sci.* **2004**, *566−568*, 1153.

(20) Kondo, T.; Mori, D.; Okada, R.; Yamamoto, S. *Jpn. J. Appl. Phys.* **2004**, *43*, 1104.

(21) Kondo, T.; Tomii, T.; Yagyu, S.; Yamamoto, S. *J. Vac. Sci. Technol., A* **2001**, *19*, 2468.

(22) Armand, G.; Lapujoulade, J.; Lejay, Y. *Surf. Sci.* **1977**, *63*, 143.

(23) Arumainayagam, C. R.; McMaster, M. C.; Schoofs, G. R.; Madix, R. J. *Surf. Sci.* **1989**, *222*, 213.

(24) Yagyu, S.; Murakami, F.; Kino, Y.; Yamamoto, S. *Jpn. J. Appl. Phys.* **1998**, *37*, 2642.

(25) Wight, A. C.; Miller, R. E. *J. Chem. Phys.* **1998**, *109*, 1976.
(26) Tomii, T.; Kondo, T.; Hiraoka, T.; Ikeuchi, T.; Yagyu, S.; Yamamoto, S. *J. Chem. Phys.* **2000**, *112*, 9052.
(27) Kondo, T.; Tomii, T.; Hiraoka, T.; Ikeuchi, T.; Yagyu, S.; Yamamoto, S. *J. Chem. Phys.* **2000**, *112*, 9940.
(28) Berenbak, B.; Zboray, S.; Riedmuller, B.; Papageorgopoulos, D. C.; Stolteb, S.; Kleyn, A. W. *Phys. Chem. Chem. Phys.* **2002**, *4*, 68.
(29) Watanabe, Y.; Yamaguchi, H.; Hashinokuchi, M.; Sawabe, K.; Maruyama, S.; Matsumoto, Y.; Shobatake, K. *Euro. Phys. J. D* **2006**, *38*, 103.
(30) Kondo, T.; Mori, D.; Okada, R.; Sasaki, M.; Yamamoto, S. *J. Chem. Phys.* **2005**, *123*, 114712.
(31) Kondo, T.; Kato, H. S.; Yamada, T.; Yamamoto, S.; Kawai, M. *J. Chem. Phys.* **2005**, *122*, 244713.

■ NOTE ADDED AFTER ASAP PUBLICATION

This article was published ASAP on March 29, 2011, with errors in Table 1 and in the Abstract, section 4.2, Discussion, and Conclusions. The correct version was reposted on June 6, 2011.